5ICEGE
5th International Conference on Earthquake Geotechnical Engineering
January 2011, 10-13 | Santiago, Chile
Paper No. SDOVA

SIMPLIFIED DESIGN OF SINGLE PILES UNDER LIQUEFACTION INDUCED LATERAL SRPEADING

Alexandros VALSAMIS[1], George BOUCKOVALAS[2], Yannis CHALOULOS[3]

WITH CORRECTED FIGURES 2 & 3
Jan. 17, 2010

ABSTRACT

Extensive damage to pile-supported structures has been witnessed in several recent earthquakes (Chi-Chi 1999, Kobe 1995, etc), as a result of liquefaction-induced large horizontal displacements of slightly sloping ground or near free-face topographic irregularities. This paper presents multi-variable design charts and relationships for the preliminary computation of maximum pile head displacement and bending moment in the case of single piles subjected to such lateral spreading of the natural ground. The charts were developed on the basis of "theory guided" statistical analysis of numerical predictions from a large number of parametric studies, where the pile–soil interraction is modelled through an advanced non linear "Beam on Winkler foundation" or *P-y* model. Three different combinations (design cases) of pile head constraints and soil conditions were considered, which are commonly encountered in practice.

Keywords: Design of piles, Liquefaction, Lateral Spreading, *P-y* method

INTRODUCTION

One of the most damaging effects of earthquake-induced soil liquefaction is the lateral spreading of soils, where large areas of ground move horizontally, to lengths ranging from some centimeters to a few meters. This phenomenon may occur in the case of even small ground surface inclination (e.g. 2÷4%) or small topographic irregularities (e.g. 2÷3m) such as those encountered at river and lake banks. In such cases, the kinematic interaction of single piles and pile groups with the laterally spreading ground may induce significant residual horizontal displacements, shear forces and bending moments to the pile, which cannot be predicted by common design methods developed for static or inertia loading transmitted from the superstructure.

From a practical point of view, two are the basic components of pile response that need to be calculated in order to avoid structural or operational failure of the foundation and the supported structure: the maximum moment M_{max} developing along the pile and the associated pile head displacement δ_{pile}. Strictly speaking, computation of M_{max} and δ_{pile} is a rather demanding task since it requires performance of 3D elastoplastic analyses of the liquefied ground response during shaking, taking also into account the interaction with the embedded piles. Such analyses are certainly possible today (Cubrinovski et al. 2008, Elgamal et al. 2006,

[1] Dr Civil Engineer, Civil Engineering School, National Technical University of Athens, Greece, e-mail: a_valsamis@hotmail.com
[2] Professor, Civil Engineering School, National Technical University of Athens, Greece.
[3] Civil Engineer M.Sc., PhD candidate, National Technical University of Athens, Greece.

Assimaki and Varun 2009, Andrianopoulos et al 2010, Valsamis et al. 2010) but are still considered well beyond limits for common applications in practice. Thus, a number of pseudo-static methodologies have been developed for simplified computations, where the loads or displacements applied by the laterally spreading ground are being estimated independently, from empirical relationships, and subsequently applied as external loads to the pile. Such pseudo-static methodologies may be divided in two categories:

- The *P-y* method, which relies upon the substitution of the ground with distributed "Winkler springs" that are governed by a non linear load-displacement (*P-y*) relationship. According to this methodology ground displacements are computed independently and then applied to the base of the springs in order to evaluate the pile deflection and the corresponding shear forces and bending moments (e.g. Tokimatsu 1999, Boulanger et al 1997, 2003).
- The limit equilibrium method, which is based on a pseudo-static estimation of the ultimate pressure applied to the pile from the laterally spreading ground. Pile displacements and bending moments can be consequently evaluated (e.g. JRA 1996, Dobry et al 2003) from elastic beam theory, or more advanced numerical analyses.

Using the first of the above methodologies, we performed a large number of parametric analyses, varying the characteristics of the piles, the boundary conditions at the pile head, as well as the ground displacements and the soil layering. The results of these analyses were consequently used to derive design charts and empirical relationships for the preliminary evaluation of maximum pile head displacements and bending moments. The statistical analysis, which was employed for this purpose, was not limited to "blind fitting" of the available data. Instead, selection of the basic problem variables and the general form of the relationships was guided by existing analytical solutions for elastic beams subjected to external loads.

SIMPLIFIED RELATIONSHIPS FROM ELASTIC BEAM THEORY

Fig. 1 shows three design cases of piles in laterally spreading ground, which are commonly encountered in practice and will be also considered herein:

(a) A 2-layer soil profile, where the liquefiable soil layer lays upon a non-liquefiable bed. To resist lateral spreading deformations, free head piles are driven through the liquefiable soil layer and firmly embedded into the non-liquefiable bed. This case is encountered in practice when river or lake banks, covered by surface alluvial deposits, need to be protected against earthquake-induced liquefaction and lateral spreading.

(b) A 2-layer soil profile, same as above, where the pile head is fully fixed, due to superstructure constraints. This case is often encountered in piles supporting bridges or other large structures, where the superstructure restrains the pile head from moving laterally and rotating.

(c) A 3-layer soil profile, where the liquefiable soil layer is encased between two non-liquefiable layers: a thin crust at the surface and a continuous bed at the bottom. In practice, the thin surface crust may consist of clayey, silty or any other liquefaction resistant soil layers, but also from unsaturated soil deposits, above the ground water table. Similar to the first configuration above, piles are driven through the liquefiable soil layer and firmly embedded into the non-liquefiable bed. The only difference lays is that the pile head is forced to move along with the surface crust, with limited (if any) relative displacement and rotation.

This categorization was considered necessary, as it is well known from conventional pile design that any constraints imposed to pile head displacement and rotation, may alter drastically the overall pile response. Note that, Ishihara & Cubrinovski (1998), Brandenberg (2002), Rollins et al. (2005) also address this

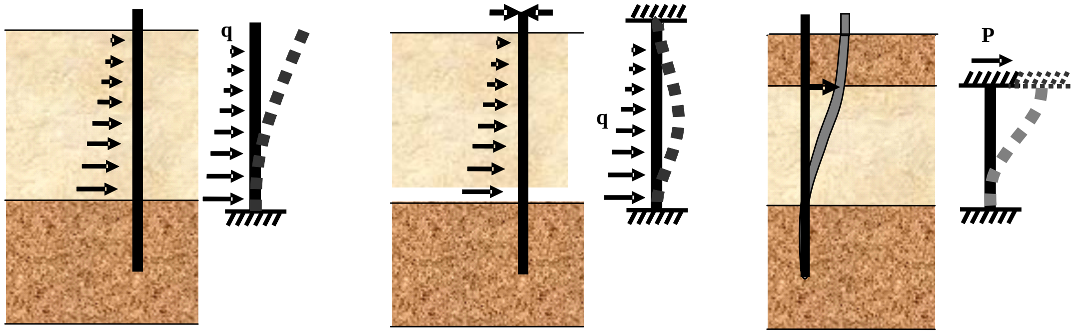

Figure 1. Typical pile-soil configurations (design cases) and corresponding simplified beam models

issue in connection with the significant effects of the pile head constraints enforced by a non-liquefiable soil crust.

In the first of the above design cases [case (*a*) in Fig. 1], the pile will respond as a cantilever beam of length equal to the thickness of the liquefiable soil layer H_{liq}, subjected to a distributed load qD (D is the pile diameter) perpendicular to its axis. Assuming that q is uniform, the analytical expressions for the pile head displacement and the maximum bending moment become:

$$\delta_{pile} = \frac{qDH_{liq}^4}{8EI} \tag{1}$$

and

$$\left|M_{max}\right| = \frac{qDH_{liq}^2}{2} = ... = 4\frac{EI\delta_{pile}}{H_{liq}^2} \tag{2}$$

In the second design case [case (*b*) in Fig. 1], the pile may be modeled as a beam with both ends fully fixed and a distributed load qD acting perpendicular to its axis. Assuming again that q is uniform, the maximum deflection of the pile, near the middle of the liquefied soil layer, and the corresponding maximum bending moment are analytically expressed as:

$$\delta_{pile} = \frac{qDH_{liq}^4}{384EI} \tag{3}$$

and

$$\left|M_{max}\right| = \frac{qDH_{liq}^2}{12} = ... = \frac{32EI\delta_{pile}}{H_{liq}^2} \tag{4}$$

Finally, in the third design case [case (*c*) in Fig. 1), the pile will act as a beam with the tip fully fixed and the head is subjected to ground displacement δ_{gr} perpendicular to the beam axis while it remains fixed against rotation. Hence, the pile head displacement should be grossly equal to the permanent ground displacement (i.e. δ_{pile}=δ_{gr}) and the analytical expression for the maximum bending moment becomes:

$$\left|M_{max}\right| = \frac{3EI\delta_{pile}}{H_{liq}^2} \tag{6}$$

Note that, the aforementioned analytical relations cannot be used directly for the estimation of expected pile displacements and bending moments, since the associated beam models are grossly approximate and they can only provide a rough identification of the factors affecting pile displacement and maximum bending moments. In reality, several additional factors should be taken into account, such as the variability with depth of the applied horizontal loads, the true (elastic-plastic) behavior of the soil, as well as several liquefaction-related phenomena such as the stick-slip nature of ground movement (Valsamis 2008, Valsamis et al. 2010). Moreover, to apply the above analytical relations for design cases (a) and (b) in Fig. 1, one should define the distributed pressure *q* acting on the pile due to liquefaction-induced lateral spreading. Although this is in principle possible, it is preferable to use the free field ground displacements as the driving force behind the pile deflection, since this quantity has been the subject of a more intensive investigation (e.g. Hamada, 1999, Youd et al, 2002, Valsamis et al., 2010) and consequently can be evaluated with greater accuracy in practice.

PARAMETRIC ANALYSES OF PILE RESPONSE

Taking into account these profound inadequacies of the available analytical methods, the response of piles embedded to laterally spreading ground was investigated parametrically, with the aid of simple numerical analyses based on the pseudo static *P-y* method, which was briefly outlined in the introduction. The choice of this methodology, instead of the equally simple methodology of limit equilibrium, was made on terms of accuracy. For instance, Ashford & Juirnarongrit (2004) concluded that the *P-y* method is the most reliable, following a thorough comparison between two commonly used limit equilibrium methods (JRA, 1996 and Dobry et al., 2003) with a modified *P-y* method that used the original curves of Reese et al. (1974) for sands, degraded with a load multiplier b = 0.1, so that the reduction in soil strength due to liquefaction is taken into account. Furthermore, based on a similar comparative study, Bhattacharya (2003) also concluded that a code proposed limit equilibrium method (JRA, 1996) is systematically non-conservative. Hence, in extend of such independent findings, the *P-y* method has been essentially established as the standard design tool in current practice, and was also chosen for the parametric analyses presented herein.

More specifically, this study relied on the *P-y* method for liquefiable soils proposed by Branderberg (2002), where the standard *P-y* curves of API (1995) for sands are degraded in terms of load P by a factor $b < 1.0$. This factor represents the effect of liquefaction on the mechanical characteristics (soil strength and deformation) of the natural soil and can be computed according to Table 1, in terms of the corrected Standard Penetration Test (SPT) blow count $N_{1,60\text{-}CS}$. Note that the aforementioned methodology has been chosen among seven (7) similar methodologies proposed in the literature (Ishihara & Cubrinovski, 1998, Cubrinovski et al., 2006, Rollins et al., 2005 & 2007, Tokimatsu, 1999, High Pressure Gas Safety Institute of Japan, 2000, Railway Technical Research Institute of Japan, 1999, and Matlock, 1970), following an extensive evaluation through comparison to three centrifuge experiments (Abdoun 1998) and one large shaking table experiment (Cubrinovski et al. 2004).

Table 1. Load degradation factors *b* for the *P-y* curves of liquefiable sand (Branderberg 2002)

$N_{1,\ 60\text{-}CS}$	<8	8-16	16-24	>24
b	0 to 0.1	0.1 to 0.2	0.2 to 0.3	0.3 to 0.5

The pile was simulated as a beam on distributed nonlinear elastic soil springs, and was analyzed numerically with the finite elements code NASTRAN (MacNeal-Schwendler Corp. 1994). While simulation of the liquefied sand layers was based on the degraded *P-y* relationships addressed in the previous paragraph, the non-liquefiable clay layers have been simulated with the *P-y* curves proposed by

API (1995, 2002), without the use of any degradation factor. It should be mentioned here that, as long as the non-liquefiable clay layers do not fail, the exact *P-y* curves which are used for their simulation do not affect significantly the results, as the associated stiffness is almost two orders of magnitude larger than that of the liquefied soil.

Based on previous experience regarding lateral spreading displacements (Ishihara and Cubrinovski, 1998, Tokimatsu, 1999, Towhata and Toyota, 1994, Valsamis et al., 2010), the displacement variation with depth of the liquefied soil was assumed to have the shape of a quarter sine, with maximum displacement at the top and zero displacement at the bottom of the liquefiable layer. On the other hand, the displacement of the non-liquefied soil layers was assumed to remain constant with the depth.

In all, one hundred sixty two (162) parametric analyses have been performed, concerning the aforementioned three different pile and ground layering combinations shown in Fig. 1. Sixty six (66) of the parametric analyses concerned the case of a 2-layer profile and a free head pile (design case *a*), an additional forty six (46) analyses have been performed for the case of a 2-layer profile and a pile with fully fixed head (design case *b*), while fifty (50) more analyses explored the case where the liquefiable soil layer is covered by a clay crust (design case *c*). These analyses were performed for the following wide range of pile and soil input parameters encountered in practice:

- Relative Density of sand Dr=35 ÷ 90 %, load degradation factor b = 0.05÷0.40 and friction angle $\varphi = 32^o \div 42^o$
- Thickness of liquefied soil layer $H_{liq} = 6 \div 10m$
- Elasticity Modulus for the pile $E = 30 \div 210$ GPa
- Pile diameter $D = 0.15 \div 0.6m$ ($EI = 16 \div 1336$ $MN{\cdot}m^2$)
- Maximum ground surface displacements $\delta_{gr} = 0.125 \div 1.20m$
- Soil crust thickness (in case c) $H_{crust} = 1 \div 4m$

DESIGN CHARTS

Pile design against lateral spreading must ensure that, following the seismic excitation (a) the pile has not sustained any structural failure (i.e. no plastic hinges have developed along the pile), and (b) the pile head displacements can be tolerated by the superstructure without any operation disruption. Hence, the following statistical analysis of the results from the parametric analyses focuses upon the maximum bending moment M_{max} along the pile and the maximum horizontal displacement δ_{pile} of the pile head. In design case *b* of Fig. 1, where the pile head is fully fixed, pile head displacements are zero, and the statistical analysis was focused upon the maximum deflection of the pile at about mid-depth of the liquefied sand layer.

Note that the depth of the maximum bending moment is in general variable. Namely, for design cases (*a*) and (*c*) in Fig. 1, maximum moments develop at the interface between the liquefied soil layer and the non-liquefied base layer, while for design case (*b*) the maximum bending moment develops near the mid-depth of the liquefiable soil layer, close to the maximum pile deflection.

Maximum Bending Moments. Following the general form of analytical expressions for the maximum bending moment obtained from elastic beam theory (Eq. 2, 4 and 6), M_{max} was correlated to the composite parameter $EI\delta_{gr} / H_{liq}^2$ which is present in the analytical expressions for all pile-soil design cases examined herein. The correlations are shown in Figs. 2a, 3a and 4a for design cases (*a*), (*b*) and (*c*) respectively. Observe that, despite the wide range of input data used for the parametric analyses, the associated data points in these figures form a fairly narrow band, a fact that essentially justifies the choice of $EI\delta_{gr} / H_{liq}^2$ as a statistical variable. A best fit line, subsequently drawn through the data points, gives the following expressions for M_{max}:

Design Case (*a*): $$M_{max} = 2.2 \frac{EI\delta_{pile}}{H_{liq}^2} \tag{7}$$

Design Case (*b*): $$M_{max} = 18 \frac{EI\delta_{pile}}{H_{liq}^2} \tag{8}$$

Design Case (c): $$M_{max} = 18 \left(\frac{EI\delta_{pile}}{H_{liq}^2} \right)^{0.65} \tag{9}$$

The similarity between the above best fit expressions with the simplified analytical solutions from elastic beam theory is indeed remarkable, especially for design cases (*a*) and (*b*) where the only difference lays in the constant multiplier of the composite term $EI\delta_{gr} / H_{liq}^2$.

Maximum Pile Displacements. In this case, the choice of the statistical variables was not as straight forward as for the maximum bending moments discussed above. The reason is that the relevant analytical relations from elastic beam theory (Eqs. 1 and 3) are expressed in terms of the applied average soil pressure q which is not readily known for the results of the parametric analyses. To overcome this obstacle, we took into account that, according to the *P-y* methodology adopted for the parametric analyses, the distributed load acting the pile axis (qD) is a function of the applied ground displacement δ_{gr}, and consequently the applied soil pressure q is related to the normalized ground displacement δ_{gr}/D. Hence, guided by the general form of the analytical solutions from elastic beam theory, and also having q replaced with δ_{gr}/D, we finally chose to correlate the following two dimensionless statistical variables: $\delta_{pile} EI / Dp_a H_{liq}^4$ representing the soil pressure applied on the pile, and $\delta_{gr} EI / Dp_a H_{liq}^4$ representing the normalized ground displacement, with p_a (=100kPa) standing for the atmospheric pressure.

The statistical correlations for the computation of maximum pile displacements are displayed in Figs. 2b, 3b and 4b for the design cases (*a*), (*b*) and (*c*) respectively. Note that the above considerations with regard to the appropriate statistical variables are only relevant to design cases (*a*) and (*b*). For design case (*c*) it is reasonable to assume that $\delta_{pile} \approx \delta_{gr}$, and consequently the correlation refers directly to these two variables.

The first thing to observe in these figures is that the data points form relative narrow bands, despite the widely different input data which were used to the derive them. As in the case of maximum bending moments, this observation comes in support of our choice of the statistical variables. Focusing next upon the correlation in Fig. 2b, for design case (*a*), it is observed that it consists of two log-log linear branches. Along the first branch, for relatively small values of the horizontal ground displacement δ_{gr}, all data points form a unique band with a steep inclination relative to the horizontal axis, while along the second

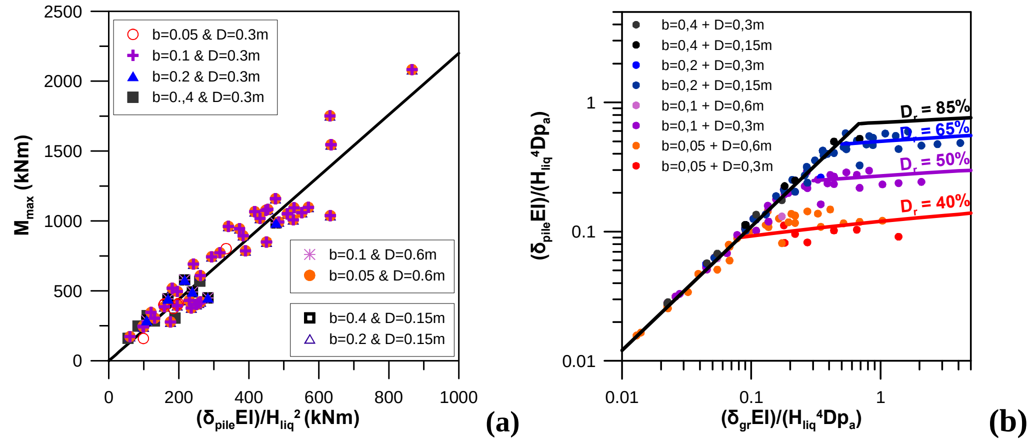

Figure 2. Design charts for (a) maximum bending moments and (b) maximum pile displacements [design case (*a*) in Fig. 1]

branch the data points are grouped according to the relative density of the liquefiable sand and form parallel bands with significantly less inclination. This characteristic shape of the chart in Fig. 2b is due to the fact that the distributed (Winkler) soil springs are elasto-plastic and thus, after a certain ground displacement, they yield. As the relative density D_r of the sands becomes higher, the onset of yielding requires larger and larger ground pressures and relative (pile-soil) displacements, thus explaining the effect of D_r displayed in this figure.

The chart in Fig. 3b, for the second design case, resembles closely the chart in Fig. 2b, only that now the ground displacements required to activate the second branch of the data points has been moved to significantly lower values. This effect may be attributed to the different constraints applied to the pile head. Namely, for the same ground displacement, fixing the pile head leads to an overall reduction of the lateral pile displacements and to a consequent increase of the relative pile-to-soil displacement which controls the *P-y* response of the soil springs. As a result, yielding of the soil springs is triggered for much smaller ground displacements δ_{gr} relative to the previous case of the free head piles.

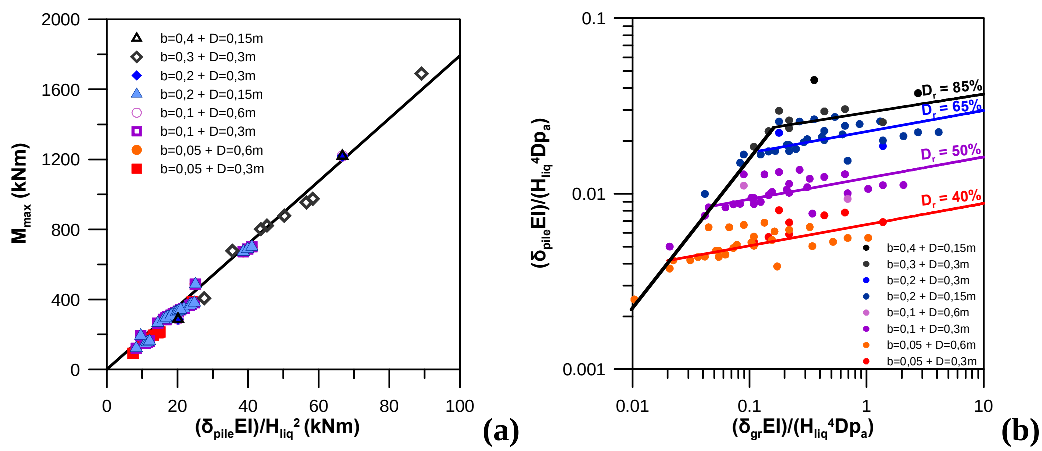

Figure 3. Design charts for (a) maximum bending moments and (b) maximum pile displacements [design case (*b*) in Fig. 1]

Finally, the chart for the 3-layer soil profile of design case (*c*) is shown in Figures 4b. In this case, the pile head follows systematically the non-liquefied soil crust displacement, being always somewhat larger, and can be approximately expressed as:

$$\delta_{pile} = 1.22\delta_{gr} \tag{10}$$

Note that this observation is also confirmed from centrifuge experiments (Abdoun, 1999), and is explained by the fact that the clay crust may be considerably stiffer than the underlying liquefied sand but does not provide a full rotation constraint to the pile head, as assumed by the simplified elastic beam representation used to gain insight to this design case.

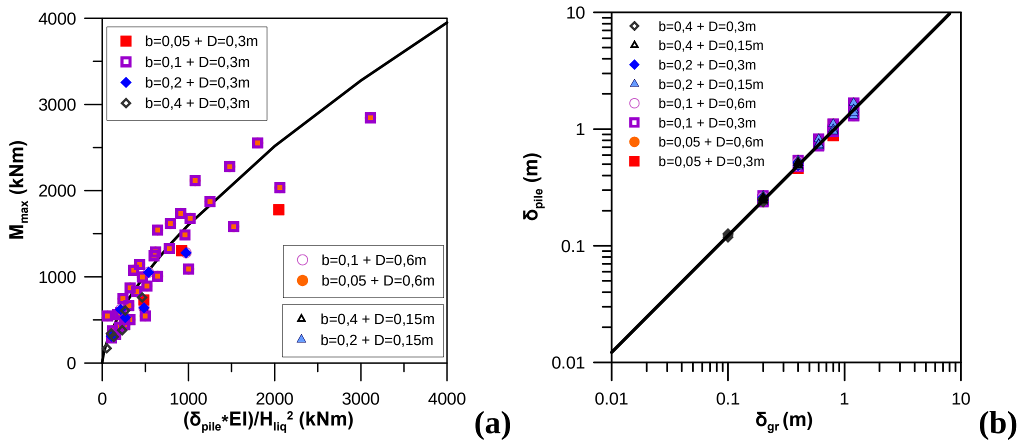

Figure 4. Design charts for (a) maximum bending moments and (b) maximum pile displacements [design case (*c*) in Fig. 1]

CONCLUDING REMARKS

In the previous paragraphs, design means were established for the approximate evaluation of the maximum displacement and bending moment of single piles subjected to liquefaction-induced lateral spreading. This task was accomplished based on the statistical evaluation of numerical predictions from a large number of parametric studies, which were performed with the pseudo-static P-y method and concern three common combinations of pile and ground conditions. Analytical solutions for simple "beam on elastic foundation" pile models proved especially valuable in identifying the basic problem parameters and in shorting out the results of the parametric analyses into simple to use design charts and empirical relationships.

The following limitations should be kept in mind when employing the results of this study in practice:

a) They were derived pseudo-statically, taking only into account the final displacement of the ground, at the end of shaking. Hence, any effects of the superstructure inertia are ignored.
b) The accuracy of pile response predictions with the proposed design means are greatly affected by the estimate of the free-field ground surface displacement. This basic input parameter should be computed conservatively, from one or more empirical relations which are published in the literature (e.g. Hamada, 1999, Youd et al, 2002, Valsamis et al., 2010).
c) The proposed design charts and relations, should be applied only when the soil has the capability to "flow" freely around the pile. In all other cases (e.g. small distance between the piles, sheet-pile wall, etc) they may lead to over-conservative pile head displacements and maximum bending moment predictions.
d) It has been assumed that the pile has been adequately embedded to the non-liquefiable base soil layer so as to guarantee fixed bottom conditions during lateral ground spreading. When this

condition is not satisfied, the constraints applied on the pile are reduced, leading to overall larger pile displacements and smaller bending moments.

AKNOWLEDGEMENTS

This study was funded by the General Secretariat for Research and Technology (GSRT) of Greece, while the Greek State Scholarship's Foundation (IKY) funded the graduate studies of A. Valsamis and Y. Chaloulos. Em. Drakopoulos, Civil Engineer M.Sc. performed a number of the parametric analyses presented above. These valuable contributions are gratefully acknowledged.

REFERENCES

Abdoun T. H. (1999) "Modeling of seismically induced lateral spreading of multi-layered soil and its effect on pile foundations", PHD Thesis, Rensselaer Polytechnic Institute, Troy, New York

Andrianopoulos K., Papadimitriou A., Bouckovalas G. (2010), "Bounding Surface Plasticity Model for the Seismic Liquefaction Analysis of Geostructures", Soil Dynamics and Earthquake Engineering, doi: 10.1016/j.soildyn.2010.04.001

API (1995), "Recommended practice for planning, designing and constructing fixed offshore platform", Washington, DC: American Petroleum Institute.

API (2002), "Recommended practice for planning, designing and constructing fixed offshore platform", Washington, DC: American Petroleum Institute.

Ashford S. A. & Juirnarongrit T. (2004), "Evaluation of force based and displacement based analyses for responses of single piles to lateral spreading", 11th International conference on Soil dynamics & earthquake engineering, 3rd International conference on earthquake geotechnical engineering, 7-9 January 2004, Berkeley

Assimaki & Varun (2009), "Nonlinear Macroelements for performance-based design of pile-supported waterfront structures in liquefiable sites", Computational Methods in Structural Dynamics and Earthquake Engineering, Rhodes, Greece, 22-24 June 2009.

Bhattacharya S. (2003), "Pile instability during earthquake liquefaction", PHD Thesis, University of Cambridge, UK.

Boulanger R.W., Kutter B.L., Brandenberg S.J., Singh P. and Chang D. (2003), "Pile foundations in liquefied and lateral spreading ground during earthquakes: Centrifuge experiments and analyses" Report No. UCD/CGM-03/01, Univ. of California at Davis.

Boulanger R.W., Wilson D.W., Kutter B.L. and Abghari, A. (1997), "Soil-pile-superstructure interaction in liquefiable sand", Transportation Research Record No. 1569, TRB, NRC, National Academy Press, 55-64

Brandenberg S.J. (2002), "Behavior of Pile Foundations in Liquefied and Laterally Spreading Ground", PHD Thesis, University of California, Davis

Cubrinovski M, Kokusho T. & Ishihara K. (2004), "Interpretation from Large-Scale Shake Table Tests on Piles subjected to Spreading of Liquefied Soils", 11th International conference on Soil dynamics & earthquake engineering, 3rd International conference on earthquake geotechnical engineering, 7-9 January 2004, Berkeley

Cubrinovski M. , T. Kokusho and K. Ishihara (2006), " Interpretation from large scale shake table tests on piles undergoing lateral spreading in liquefied soils" Soil Dynamics and Earthquake engineering, vol.26

Cubrinovski M., Uzuoka R., Sugita H., Tokimatsu K., Sato M., Ishihara K., Tsukamoto Y., Kamata T. (2008), "Prediction of pile response to lateral spreading by 3-D soil-water coupled dynamic analysis:

Shaking in the direction of ground flow", Soil Dynamics and Earthquake Engineering Volume 28, Pages 421-435.

Dobry, R., Abdoun, T., O' Rourke T.D., Goh S.H. (2003), "Single piles in lateral spreads: Field Bending Moment Evaluation", ASCE Journal of Geotechnical and Geoenvironmental Engineering, Vol. 129, No. 10, October, pp. 879–889

Elgamal A., He L., Abe A., Abdoun T., Dobry R., Sato M., Tokimatsu K., Shantz T. (2006), "Liquefaction-induced Lateral Loads on Piles", 4th International Conference on Earthquake Engineering, Taipei, Taiwan, October 12-13, 2006.

Hamada M. (1999), "Similitude law for liquefied-ground flow", Proceedings of the 7th U.S.-Japan Workshop on Earthquake Resistant design of lifeline facilities and countermeasures against soil liquefaction, pp. 191-205.

High Pressure Gas Safety Institute of Japan (2000), "Design method of foundation for Level 2 earthquake motion", (In Japanese)

Ishihara K. & Cubrinovski M. (1998), "Soil-pile interaction in liquefied deposits undergoing lateral spreading", XI Danube-European Conference, Croatia, May 1998

Japan Road Association (1996), "Specifications for highway bridges", Part V Seismic Design

The MacNeal-Schwendler Corporation (1994), "MSC/NASTRAN for Windows: Reference Manual"

Matlock, H. (1970). "Correlations of design of laterally loaded piles in soft clay." Proc. Offshore Technology Conference, Houston, TX, Vol 1, No.1204, pp. 577-594.

Railway Technical Research Institute (1999), "Earthquake resistant design code for railway structures", Maruzen Co. (in Japanese)

Reese L.C. and Van Impe W. F. (2001), "Single piles and pile groups under lateral loading", A.A. Balkema/Rotterdam/Brookfield, Book p.p.463.

Rollins K.M, Gerber T.M., Lane J.D. and Ashford S.A. (2005), "Lateral resistance of a full-scale pile group in liquefied sand", ASCE Journal of Geotechnical and Geoenviromental Engineering, Vol 131, No. 1, January, pp. 115-125.

Rollins K.M., Bowles S., Brown D. & Ashford S. (2007), "Lateral load testing of large drilled shafts after blast-induced liquefaction", 4th International Conference on Earthquake Geotechnical Engineering, Paper no 1141, June 25-28, Thessaloniki, Greece

Tokimatsu K. (1999), "Performance of pile foundations in laterally spreading soils", Proc. 2nd Intl. Conf. Earthquake Geotechnical Engineering (P. Seco e Pinto, ed.), Lisbon, Portugal, June 21-25, Vol 3, pp. 957-964

Towhata I. & Toyota H. (1994), "Dynamic analysis of lateral flow of liquefied ground", Proc. 5th U.S.-Japan Workshop on Earthquake Resistant Design of Lifeline Facilities and Countermeasures Against Soil Liquefaction, Tech. Rep. NCEER-94-0026, T. D. O'Rourke and M. Hamada (eds), November 7, pp. 377-387

Youd L. T., Hansen M. C. and Bartlett F. S. (2002), "Revised multilinear regression equations for prediction of lateral spread displacement", Journal of Geotechnical and Geoenvironmental Engineering, Vol. 128, No. 12, December 1, pp 1007-1017.

Valsamis A., Bouckovalas G. & Papadimitriou A, (2010), "Parametric investigation of lateral spreading of gently sloping liquefied ground", Soil Dynamics and Earthquake Engineering Volume 30, Issue 6, Pages 490-508

Valsamis (2008), "Numerical simulation of single pile response under liquefaction-induced lateral spreading", Doctorate Thesis, Department of Geotechnical Engineering, School of Civil Engineering, National Technical University of Athens.